



Numerical analysis of surface settlement with saturated zone during urban tunnelling

Ganesh S. Ingle^{*1, a}, Shailendra Banne^{2, b}, Darshan Gaidhankar^{1, c}, Kshitij Dhawale^{1, d}, Dinesh Aswar^{3, e}

¹Department of Civil Engineering, Dr. Vishwanath Karad MIT World Peace University, Pune, India

²Department of Civil Engineering, Pimpri Chinchwad College of Engineering, Pune, India

³Nicmar University, Pune, India

Article Info

Abstract

Article History:

Received 19 Dec 2024

Accepted 18 Feb 2025

Keywords:

Surface settlement;
Analytical method;
Rocscience;
Water pocket;
Urban tunnelling

Surface settlement assessment during urban tunnelling, especially in the presence of saturated bodies, is crucial for the safety of nearby structures and utilities. This study uses a finite element-based Rocscience (RS2) tool to obtain the surface settlement trough for the two cases, viz. tunnel hits a water pocket (saturated body) and grouted water pocket. In the case of tunnel hits a water pocket, the maximum surface settlement was found to be 31.6 mm, while for the grouted water pocket, it was 16.4 mm, which is nearly 50% less than the latter case. Furthermore, the support capacity curve findings showed that the support lining is unstable when the tunnel hits a water pocket; however, in the grouted water pocket case, the liner's safety exceeds the design factor of safety. In addition, the combined maximum surface settlement obtained by the numerical method (RS2) is validated with the O'Reilly and New method, based on Peck's classical empirical theory. It is found to be closer to it by 6%, indicating good agreement. The findings are also compared with a few analytical studies, including Limanov's, Sagaseta's and the Gonzales-Sagaseta method. Limanov's and Sagaseta's, methods showed comparable results to the present study; however, the Gonzales-Sagaseta method underestimated the results. Finally, the applicability of the RS2 method is verified by conducting the parametric study on tunnel geometry (depth and diameter), and the results compared to analytical methods. The application of predicted surface settlement guides the tunnel engineer from the future consequences regarding the destructive effects of adjacent structures and facilities, particularly in the presence of water bodies.

© 2025 MIM Research Group. All rights reserved.

1. Introduction

Tunnel projects are inherently dangerous due to the variability and unpredictability of geological conditions [1]. Tunnel construction, particularly in hilly areas, is mainly associated with complex geology and uncertainties [2]. The uncertainties in geology and hydrogeology make tunnelling very challenging. Groundwater and saturated zones are the main origins of tunnel-building issues that allow water to enter into the tunnel. Because the pressure at the excavation boundary is typically atmospheric, the tunnel function as a groundwater drain [3]. The effects of it create various problems, such as unfavourable working conditions, damage to construction equipment's, increases in the construction period, and, most notably, property losses and casualties [4,5]. Therefore, the likelihood and potential extent of water bodies, as well as the intensity of flow during tunnel construction, must be predicted in advance [6]. However, this problem may occur because of a lack of accurate information regarding the location of saturated zones/water bodies, due to

*Corresponding author: ganesh.ingle@mitwpu.edu.in

^aorcid.org/0000-0002-2203-0011; ^borcid.org/0000-0001-5626-5508; ^corcid.org/0000-0003-0029-6019;

^dorcid.org/0009-0008-7051-2446; ^eorcid.org/0000-0002-5540-987X

DOI: <https://dx.doi.org/10.17515/resm2025-571st1219>

inadequate geotechnical investigations and squeezing ground conditions [4]. Therefore, prior to the construction, assessment or prediction of saturated zones/water bodies is crucial for the design and stability of tunnels [7].

Groundwater control is the prerequisite for the effective completion of tunnels [8]. Due to the saturated type of geology, India has experienced the worst disaster in the history of tunnelling. The accidental case studies, such as Bihar Chass-Nala colliery disaster, Kolkata East-West metro bowbazar accident, an artesian blowout in the Tunnel Boring Machine (TBM) driven in Dul Hasti J&K, groundwater ingress in head race tunnel of Tapovan: Vishnugad Hydroelectric Project in higher Himalayas etc. The unwanted entry of groundwater flows in the excavation area results in groundwater drawdown. This could result in ground settlement in addition to the settlement caused by the excavation effect [9,10,11,12] as well as some other environmental impacts [13]. The result of groundwater drawdown caused more than 1m ground subsidence during the construction of the Romeriksporten tunnel in Norway. Another case study reported by Yoo et al. [14] in which typical excavation under an active airport in water-bearing permeable ground resulted in significant ground surface settlements of nearly 200 mm excess on the apron area due to insufficient groundwater control. Despite the fact that the pre-grouting was carried out along the tunnel's periphery, this occurred.

The case studies discussed above highlight the significance of groundwater and settlement control during tunnelling operations in ground-water drawdown conditions [10,15]. Whereas a limited number of studies [16,17,18,19], have been conducted to characterize the ground surface settlement produced by tunnelling in water-bearing ground/saturated zones. Yoo [10] carried out a thorough investigation into the interaction of tunnelling and groundwater during tunnelling in a saturated stratum. Shen et al. [20] also did a detailed investigation on the long-term settlements behaviour of metro tunnel and found that it is caused by adjacent construction and groundwater penetration. Some of the studies [21,22,23,24] are not related to tunnelling but focuses on the lasting ground sinking instigated by dewatering in the Shanghai area. All of these scenarios demonstrate the importance of evaluation of groundwater study for proper treatment and ensuring long-term tunnel stability [7,25,26].

In fact, various methods have been used to evaluate the ground water into the tunnel. The most common are analytical, empirical, semiempirical, and numerical. Because of their simplicity, numerous analytical studies are used to compute the quantity of underground water seepage into the tunnel [5]. These studies are based on the assumption of homogeneous and isotropic rock permeability [26]. Numerical methods are complex and time-consuming in nature; despite these limitations, numerical methods have been used as a primary tool in most of the available studies because they provide more accurate results than the analytical method [5,10]. The numerical techniques can be used to simulate the heterogeneous and anisotropic conditions, as well as the interaction between groundwater and underground excavations [26]. Furthermore, the advancement in computer computational performance has resulted in the significant use of numerical techniques in tunnel engineering [13, 27]. Many numerical methods employ the finite element approach [28,29], while few studies are based on the boundary element methods, where only elements at boundaries are considered [30,31].

It is observed that numerous studies have been carried out by numerical method in tunnel engineering; this may be to obtain the tunnel- induced settlements, tunnel support stability, TBM performance, geological conditions, tunnel convergence, etc. [32]. However, the quantum of research that has been conducted to characterize the ground surface settlement trough produced by twin tunnelling, especially for water-bearing ground/saturated zones, is limited. Further numerical studies are required for predicting the ground surface settlement, especially for the saturated zone/ground. Also, the majority of the research has been conducted outside India; to investigate the impact of TBM tunnelling on Indian ground conditions, more studies/investigations are required.

The primary goal of the present study is to apply the Rocscience (RS2) tool to predict the surface settlement trough in case of twin tunnelling for two cases: when the tunnel (TBM) hits the A) hypothetical saturated zone/water pocket positioned near the 2nd tunnel crown and B) after

grouting the saturated zone (grouted water pocket). The RS2 results are validated using the empirical approach suggested by O'Reilly and New [33] and also compared to a few other analytical approaches. Finally, the applicability of the RS2 method is verified by conducting the parametric study on tunnel geometry (depth and diameter), and the results are compared with analytical methods.

2. Methodology

This study explains the investigation of surface settlement caused by urban tunnelling in the presence of a saturated body (water pocket). Fig.1 represents the detailed framework and overall approach used in the study. A thorough review of literature was carried out prior to decide the objectives of the work. Regional geology and its properties are hypothetically assumed. Twin tunnel geometry and its support system was assumed to be a composite lining consisting of a circular segmental lining as a primary support and a cement grouting layer as a secondary support by the middle and tail shield of TBM. The properties of segmental lining and steel are also assumed.

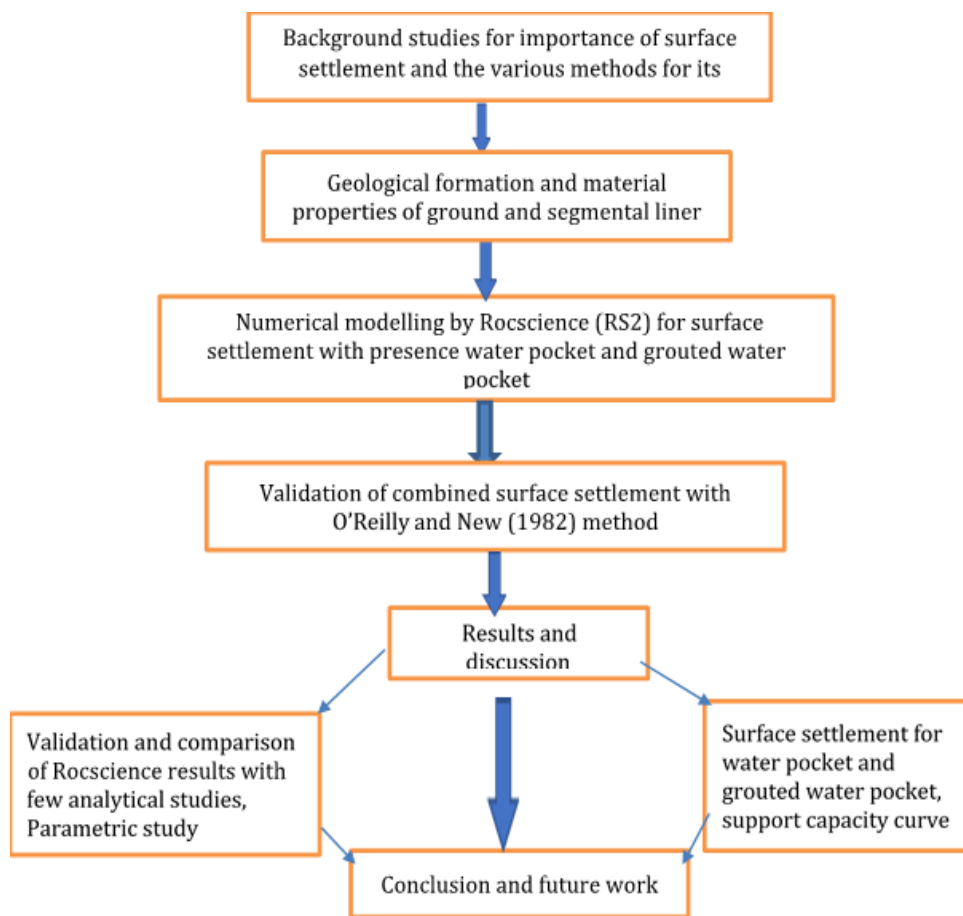


Fig. 1. Framework of the study

The surface settlement analysis was carried out in three steps. a) Numerical analysis was carried out using the FEM-based Rocscience tool (RS2) for the cases of tunnel hits to the water pocket and grouted water pocket. b) The numerical method result (combined surface settlement trough) of the grouted water pocket was validated with the empirical approach proposed by O'Reilly and New method [33], c) the numerical method result was further compared with a few analytical approaches including, Limanov's, Sagaseta's, and the Gonzales-Sagaseta method. Limanov's and Sagaseta's methods. Finally, conclusions were drawn with the comparison of numerical method with empirical and analytical methods.

3. Geology and Material Properties

Geology is one of the basic and most important aspects on which the whole tunnel support system is decided. In this study, a 2D finite element model was performed on hypothetical 5.8m diameter circular twin tunnel positioned 20m below the ground surface. The geological formation consists of eight soil layers up to 40 m depth with an average unit weight of 17kN/m³. The borehole of the geological formation, its thickness, and the location of the tunnel are shown in Fig. 2. The borehole log data is closely related to the East-West Metro and the heritage structures in Kolkata, India.

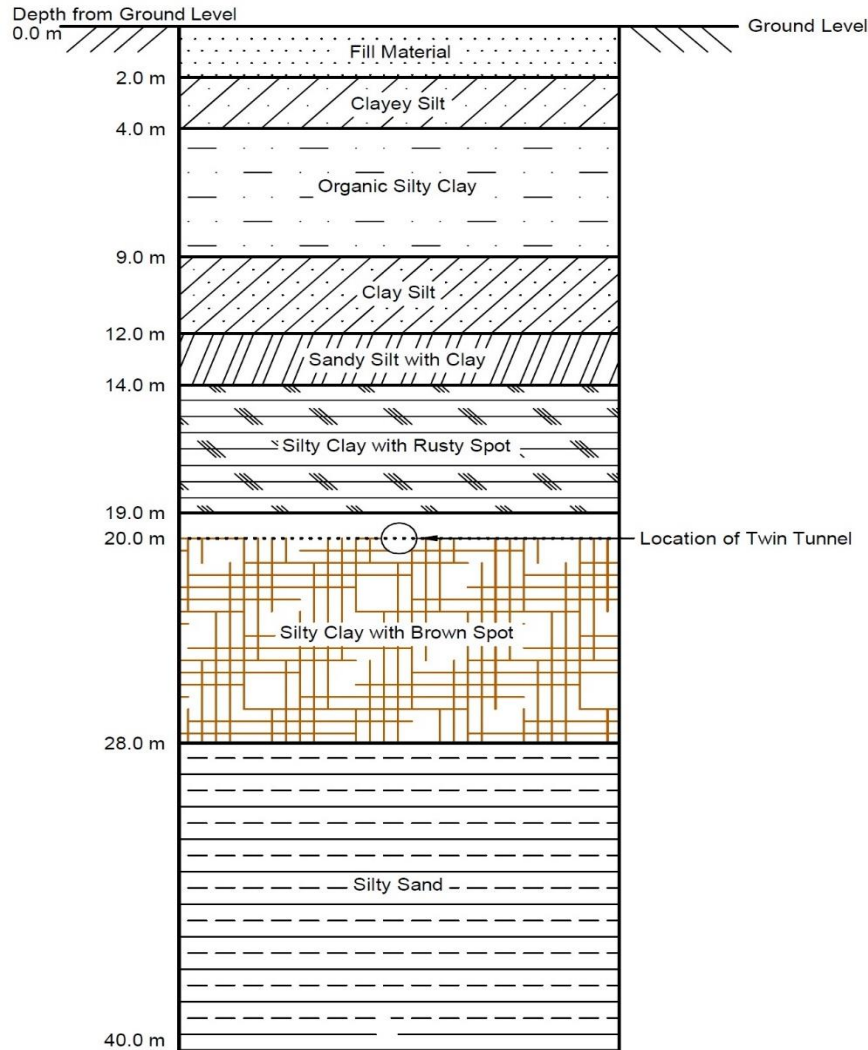


Fig. 2. Borehole of geological formations

The borehole data consists of the fill material as a topmost layer with a 0-2 m thickness below the ground surface. The second layer is clayey silt from 2 to 4 m thick, followed by organic silty clay up to 9 m thick. The clay-silt with calcareous nodules, sandy-silt with clay, and silty clay with rusty spots (loamy sandy deposits of various origins) are located at 9 m, 12m, and up to 14 m depths, respectively. In the present study, twin tunnels are considered (closely related to the East-West Metro Kolkata, India), which are located at 20 m depth below the ground level and positioned between the sixth and seventh soil layers. These layers consist of silty clay with rusty spots and silty clay with brown yellow-spots (loess), and extend up to a depth of 28 meters. The bottommost layer below 28 meters is silty sand. Table 1 shows the soil layer configuration and its elastic as well as engineering properties.

Table 1. Elastic and engineering properties of soil configuration

Soil	Soil classification	Unit Wt. (kN/m ³)	Cohesion (kN/m ³)	Friction angle (degree)	Young's Modulus (MPa)	Poisson's ratio	Permeability (m/s)	Porosity
Fill material	-	18.5	0	26	10	0.2	5 X 10 ⁻⁵	0.5
Clayey silt	CL	18	0	28	15	0.3	1 X 10 ⁻⁷	0.5
Silty clay with organic materials	OL	17	0	28	25	0.3	1 X 10 ⁻⁷	0.5
Clay-silt with trace of calcareous modules	OH/OL	19	5	28	40	0.3	1 X 10 ⁻⁷	0.5
Sandy-silt with occasional clay	SM/SC	18.5	4	30	55	0.3	5 X 10 ⁻⁷	0.5
Silty clay with rusty spots	SM	19.5	5	32	63	0.3	1 X 10 ⁻⁷	0.5
Silty clay with brown spots	ML/CL	19.5	5	32	65	0.3	1 X 10 ⁻⁷	0.5
Silty sand	SM	19.5	0	34	100	0.3	1 X 10 ⁻⁷	0.5

Table 2. Properties of concrete and steel

Parameters	Value
Type of Concrete	M50
Compressive strength (MPa)	50
Material Safety Factor	1.5
Characteristic Tensile Strength (MPa)	4.69
Design Tensile Strength (MPa)	4.15
Modulus of Elasticity shorty term or (Elastic Modulus) (MPa)	35,355
Poisson's Ratio	0.15
Unit Weight of Reinforced Concrete (MPa)	25
Steel Grade	Fe500
Characteristic Steel Strength (MPa)	500
Material Safety Factor	1.15
Design Steel Strength (MPa)	435
Ultimate Steel Strength (MPa)	545
Modulus of Elasticity (MPa)	200,000

To prepare the Rocscience (RS2) model, the tunnels are assumed to be supported by a composite lining consisting of a circular segmental lining as a primary support and a cement grouting layer as a secondary support by the middle and tail shield of TBM. The composite circular tunnel lining is made up of a 275 mm thick universal segmental ring and a 150 mm thick TBM grout. A segmental ring has an internal diameter of 5800 mm and an external diameter of 6350 mm. The space between

the tunnel excavated diameter and the outer diameter of the segmental ring is filled with Cementous grout and the sodium silicate mixture for the circular secondary lining from TBM's tail shield. Table 2 shows the properties of segmental lining and steel.

4. Numerical Modelling Using Rocscience (RS2)

In this study, numerical analysis was performed using a 2D finite element program, Rocscience (RS2). RS2 can be used to analyze and design tunnels and the support system. In the present work, the RS2 is used to predict the surface settlement trough for two cases: when the TBM hits A) the hypothetical saturated zone/water pocket positioned near the 2nd tunnel crown, and B) the grouted water pocket (after grouting the saturated zone). Fig. 3 depicts the tunnel FEM model in the presence of a water pocket/saturated zone, and Fig. 4 represents the model of twin tunnel after grouting the water pocket/saturated zone, called a grouted water pocket.

The models consist of twin tunnels with internal segment ring diameters of 5.8 m and a distance of 15m c/c. The overburden of buried tunnel is 20 m and subjected to a surface load of 40 kN/m². The two extreme-sided boundaries are considered at eight times the diameter of the tunnel from the tunnel centerline. The top surface is a free boundary condition, whereas the bottom surface is fixed to allow for vertical movement whereas the right and left edges of the external boundary are fixed in the X direction. The soil layers are discretized using triangular elements with three nodes and a gradation factor of 0.1. To determine the optimal mesh size, a sensitivity analysis was conducted on the mesh, which ensured accurate results while maintaining computational efficiency. A graded mesh was applied across all models, with finer mesh elements near the tunnel opening (regions of high-stress gradients) and became coarser towards the model boundaries.

In the present study, the soil layers behavior is assumed to be elasto-plastic material, and the Mohr-Coulomb (MC) model shows perfectly linear elastic-plastic behavior. It is well known that the Mohr-Coulomb failure criterion is not able to accurately reproduce the soil movements induced by excavation because it represents Young's modulus of soil in the in-situ stress state [34]. Nevertheless, most of the finite element-based numerical studies are still performed using simple constitutive models such as Mohr-Coulomb (MC). Because of the simplicity of formulation, it has more applications than other models, as well as MC model requires a limited number of input parameters determined by simple tests [35], and the calculation times tend to be lower than those of advanced soil models [36,37,38,39].

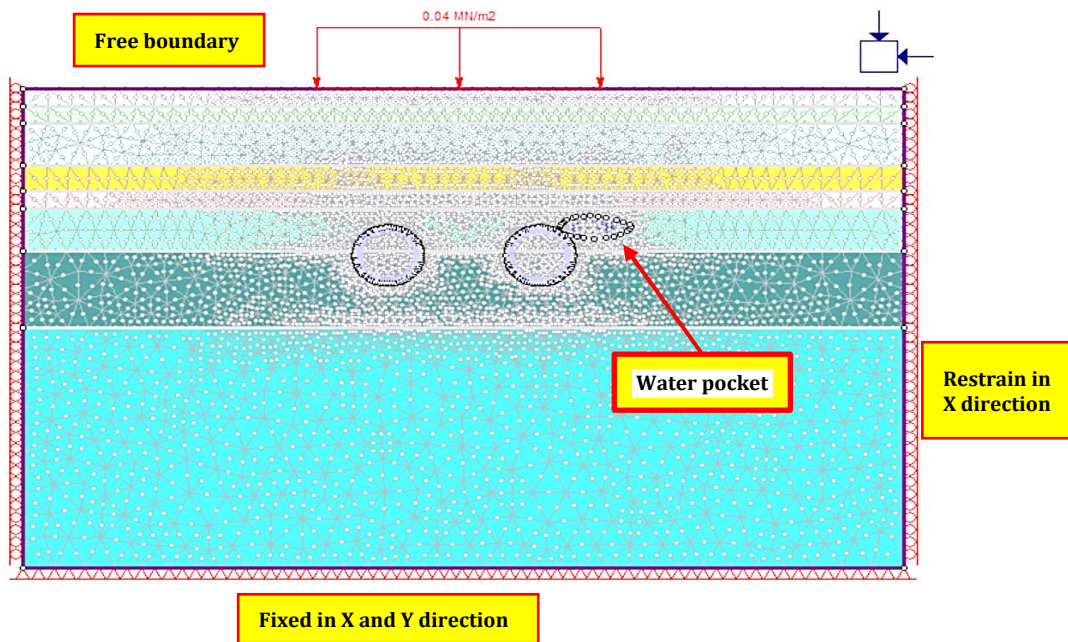


Fig. 3. FEM model in presence of water pocket (case A)

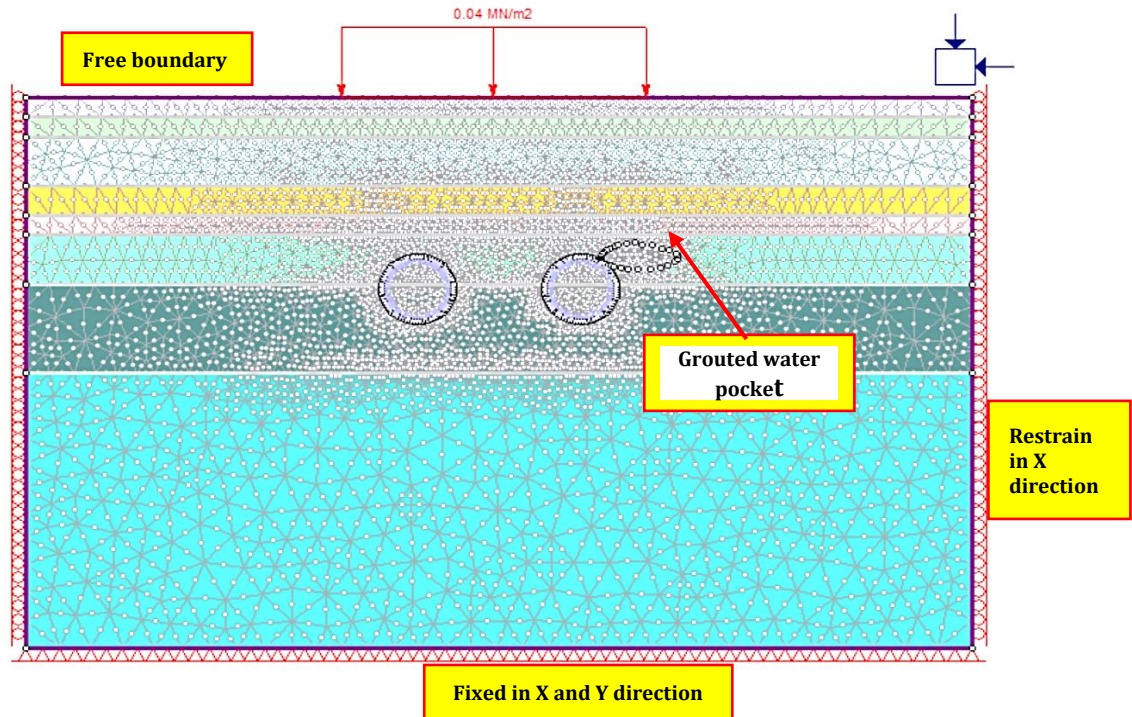


Fig.4. FEM Model in presence of grouted water pocket (case B)

The water table is considered to be 23 m below the ground surface. In the present study, the soil layers are assumed to be in undrained condition, and the short-term settlement analysis was carried out, which is mainly contributed to by construction methods. [40,41]. Settlement due to consolidation was neglected. The RS2 model considers the undrained strength and stiffness parameters, whereas the undrained Young's modulus was back-calculated based on effective shear modulus. Hence, no pore water pressure will be generated.

4.1. Modelling and Construction Sequence

The first model, case A (Fig. 3), considers a hypothetical unknown water pocket of 6 m long and 2 m thick located at the upper right corner of the 2nd tunnel. The average depth of water pocket is 14 m below the ground level. The water inside the pocket was modelled as an elastic material with a unit weight of 9.81 kN/m³, a Poisson's ratio of 0.499, and Young's modulus of 1.1 GPa.

Table 3. Various construction stages and their features

Construction sequence	Features
Initial condition, initial ground stress	The effective stress ratio in and out of plane is considered 1.0
Excavation of 1 st tunnel	The induced load factor of 0.95 from inside the tunnel, indicates 5% stress relaxation by TBM
Composite lining of 1 st tunnel	combination of the primary lining (Segments) and secondary lining (grout)
Excavation of 2 nd tunnel	The induced load factor of 0.95 from inside the tunnel, indicates 5% stress relaxation by TBM
Tunnel hit to water pocket	A water pocket of 6 m long and 2 m thick is located at the right top of 2 nd tunnel, which is filled with water and loose soil. As the 2 nd tunnel hits a water pocket at the tunnel crown, water will start entering the tunnel, causing a huge volume loss in the water pocket. This volume loss creates an empty cavity with no support, which eventually links to a huge settlement at the ground surface
Composite lining of 2 nd tunnel	combination of the primary lining (Segments) and secondary lining (grout)

In the second model, case B (Fig. 4), the tunnelling was carried out after grouting the water pocket using a grouting technique having a unit weight of 24 kN/m³ and a friction angle of 31 degrees. The composite tunnel lining consists of 275mm thick segmental lining and 150 mm thick grout, which is assumed to be an elastic material with minimal seepage loss during tunnel construction. TBM grout loss during secondary lining around the tunnels is not considered. The surface settlement for both cases was determined for the following construction sequences/stages, which are presented in Table 3.

In most of the previous studies, the stress relaxation factor has been determined based on no scientific reason and merely as a hypothetical choice [42]. In contrast, the relaxation factor depends on various factors such as tunnel geometry, initial stress, soil properties, depth of the tunnel, and the length of the unsupported section at the tunnel heading. Near the working face, it is almost zero, and behind the tunnel face, it varies from 0 to 1 [42,43]. Smaller values of the relaxation factor represent smaller deformations and larger forces in the lining. In the present study, the composite lining is used behind the tunnel face, which simulates the smaller deformation and greater forces in the lining; hence the smaller stress relaxation factor is considered, i.e. 5%, and the induced load factor is 0.95.

5. Results and Discussion

The RS2 was used to analyze the tunnel surface settlement in the presence of a water pocket. For tunnel hits to the water pocket (case A) and grouted water pocket (case B), the total surface settlement and its variation along the lateral distance are obtained. The results of the grouted water pocket (case B) were validated using the empirical method suggested by O'Reilly and New [33] and compared with a few analytical approaches.

5.1. Surface Settlement in the Presence of Water Pocket

During the various construction stages, the maximum surface settlement and its variation along the horizontal distance are computed. Fig.5 shows the results of surface settlement/displacement observed for one of the construction stages namely tunnel hits to the water pocket.

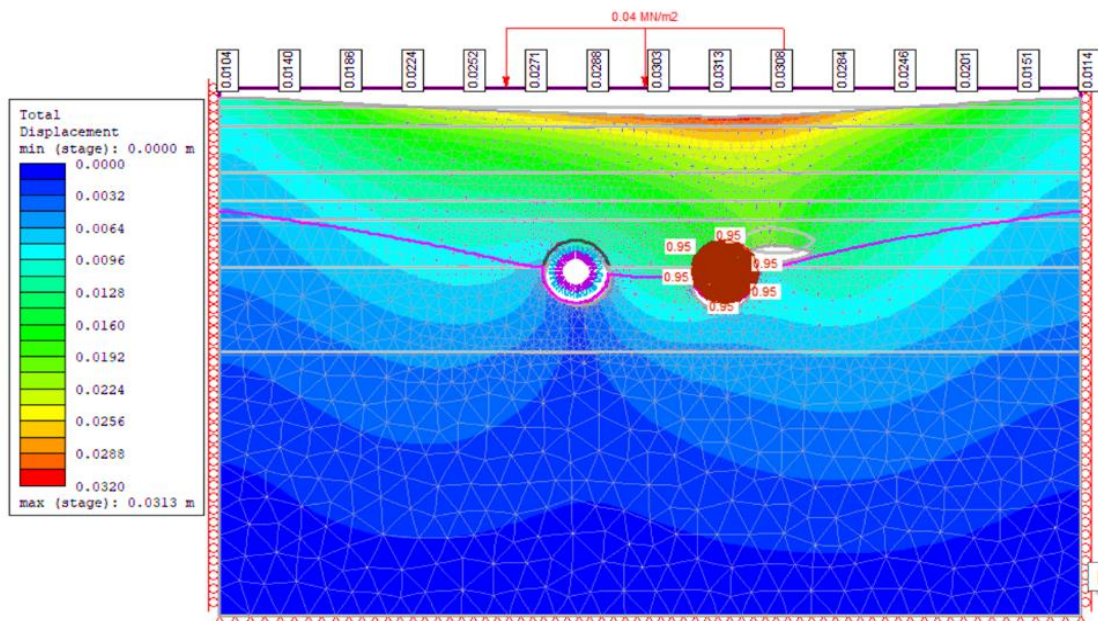


Fig. 5. Settlement at ground surface after TBM hits a water pocket

Table 4 shows the magnitude of maximum surface settlement at various construction stages for both cases. In the case of tunnel hits to a water pocket, it was found that the surface settlement of 30.3 mm occurred during the excavation stage of 2nd tunnel and that of 31.6 mm when the tunnel hits the water pocket. The maximum surface settlement was increased by 5% as compared to the

2nd tunnel excavation stage. This may be because entry of water in to the excavation area increases the effective stress and consequently increases the surface settlement.

Table 4. Maximum surface settlement for various construction stages for both the cases

Excavation stages	Surface settlement (mm)	
	Tunnel hits a water pocket	Tunnel hits a grouted water pocket
Initial (in situ) condition	0.00	0.00
Excavation of 1 st tunnel	29.1	18.8
Composite lining of 1 st tunnel	25.2	14.7
Excavation of 2 nd tunnel	30.3	18.6
Tunnel hit to water pocket	31.6	16.4
Composite lining of 2 nd tunnel	29.2	14.02

While, in the case of a grouted water pocket, the maximum surface settlement was 16.4 mm, which is nearly 50% less than the presence of water. This may be because of the pre-grouting effect of the water pocket, which controls the drawdown above the tunnel and reduces the effective stress, results in a decrease in the settlement. In both cases, the application of lining to the 2nd tunnel decreased the surface settlement; this may be because of the reduction of water flow quantity in the excavation area due to the placement of composite lining. The effect of composite lining provides superior watertightness and load bearing capacity [44]; hence the provision of composite lining applies a sufficient face pressure to push the flow towards the ground surface and reduce the water flow quantity in the excavation area.

Figs. 6 and 7 show the variation of total surface settlement (displacement) with lateral distance in cases A and B, respectively. In both cases, the surface settlement variation with horizontal distance follows a similar pattern, i.e., as the distance increases, the settlement increases as well, reaching a maximum at the crown of 2nd tunnel and further decreasing for the increment of horizontal distance.

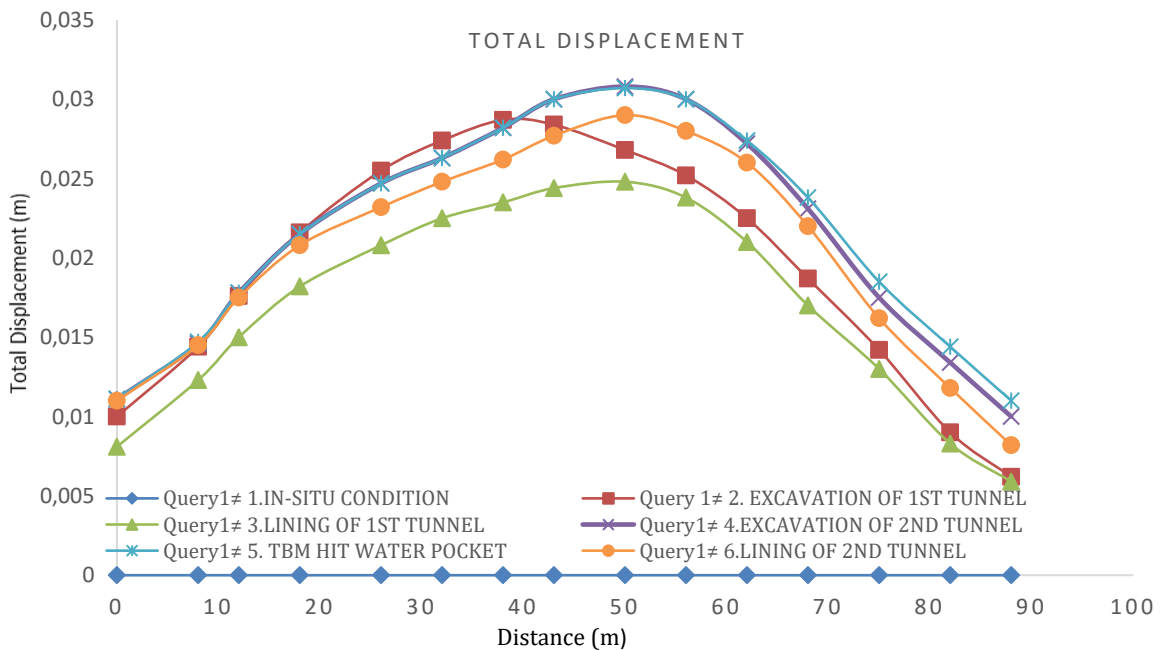


Fig. 6. Ground surface settlement variation with horizontal distance for different construction stages (case A- tunnel hits a water pocket)

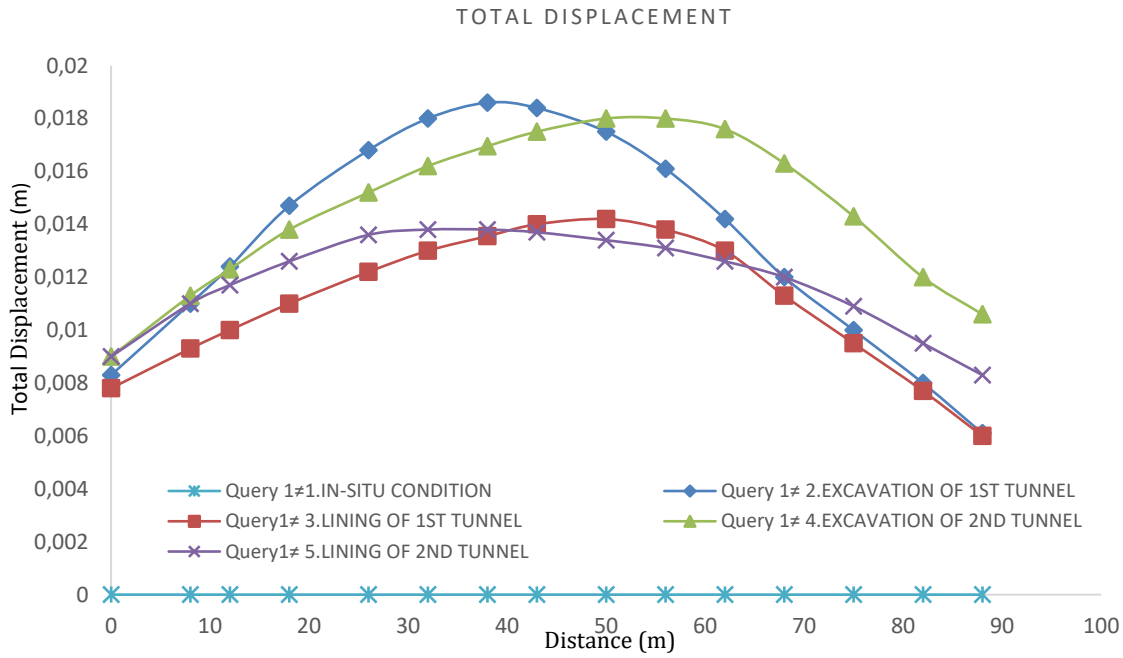


Fig. 7. Ground surface settlement variation with horizontal distance for different construction stages (case B- tunnel hits a grouted water pocket)

Fig. 6 shows the wider and deeper settlement trough, whereas Fig.7 shows a narrower and shallower settlement trough. This clearly shows that grouting a water pocket has a positive effect on settlement trough that are considerably narrower and shallower, with a maximum settlement of nearly 50% less than the presence of water. In the presence of a water pocket, the maximum surface settlement is observed to be 31.6 mm, which is a red trigger as it exceeds the prescribed limits (20mm) laid by EURO, the Chinese code, and British practices [45-46], causing the surface structures to be unsafe.

5.2. Support Capacity Curve

Tunnel support capacity curves are self-generated by the Rocscience program. These are the capacity envelopes of shear force, axial force, and bending moment, which provide the factor of safety of lining (concrete liner and steel sets). Figs. 8 and 9 depict the support capacity curves for cases A and B respectively.

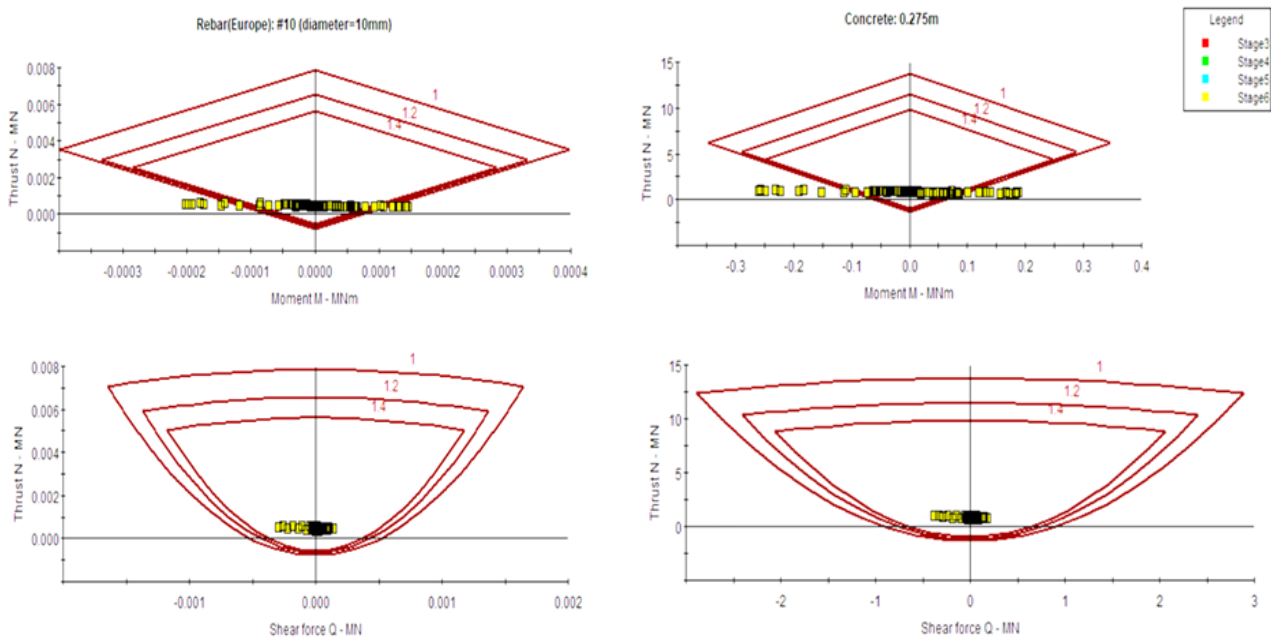


Fig. 8. Support capacity curve for case A – presence of water pocket

In the present study, the tunnels are assumed to be supported by a composite lining consisting of a circular segmental lining as a primary support and a cement grouting layer as a secondary support by the middle and tail shield of TBM. Figs. 8 and 9 show the relationship between thrust and moment, as well as thrust and shear force, which represent the liner stress and strength envelopes for both cases, respectively. This allows for the stresses induced in segmental liners and is easily envisioned in terms of strength envelopes and safety factors. The Carranza-Torres and Diederichs method is used to plot the three safety envelope factors, 1, 1.2, and 1.4, which ensure the tunnel support stability.

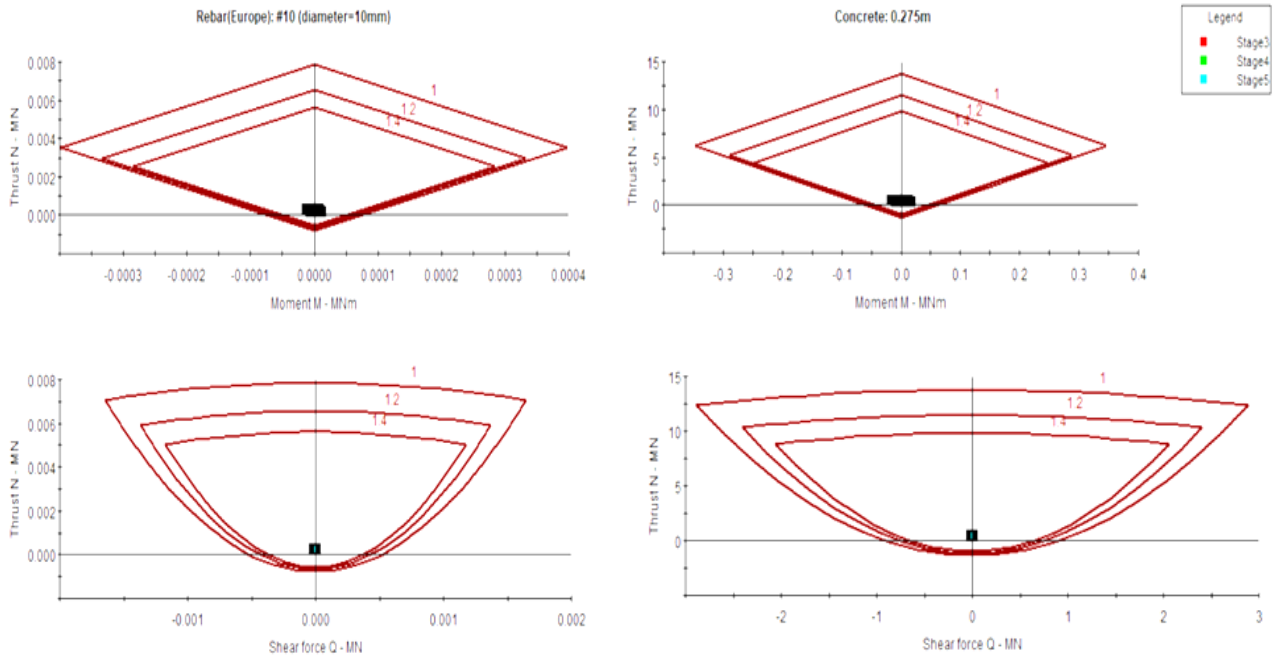


Fig. 9. Support capacity curve for case B – grouted water pocket

When the tunnel hits a water pocket, in a few stages the point nodes fall outside the envelope (Fig.8) indicating that their factor of safety is smaller than the envelope value. These findings suggest that the support lining is unstable during the stage when the tunnel hits the water pocket (saturated body), which may affect the instability of tunnel supports and the crown. For case B, Fig.9 shows that the point nodes are lying within the envelope (inside the envelope) of a factor of support safety of 1, 1.2, and 1.4 at all stages, indicating that their factor of safety is more than the envelope value. It is found that the liner’s safety exceeds the design factor of safety. This demonstrated that after the water pocket is grouted, the tunnel segmental lining support will be safe.

5.3 Validation Using O’Reilly and New method

In this study, the empirical equation proposed by O’Reilly and New [33] is used to validate the results obtained by the numerical method RS2 for the case of grouted water pocket. O’Reilly and New method is based upon the first classical empirical method developed by Peck (1969) [47], which is a well-known as Gaussian distribution method. Various empirical methods, such as Attewell et al. (1986), [16], Hansmire and Cording (1972) [48], O’Reilly and New (1982) [33], Wang et al. (2016) [49] are based upon the hypothesis presented by Peck [47] but the O’Reilly and New method is widely used as a regression method and is especially used to predict the transverse surface settlement trough produced by the twin tunnels. The equation proposed by O’Reilly and New method is illustrated below;

$$S = S_{\max} \left[e^{-\left(\frac{x_1^2}{2.i^2}\right)} + e^{-\left(\frac{(x_1-d)^2}{2.i^2}\right)} \right] \quad (1)$$

where, S - Theoretical settlement curve; d - Lateral c/c distance between the two tunnels; x_1 - Lateral distance from the first bored tunnel center-line; S_{max} - Maximum settlement (short-term) at the tunnel centerline (m). S_{max} is calculated by using the following equation (2)

$$S_{max} = 0.313x \frac{V_L x D^2}{i} \tag{2}$$

Where; V_L - Volume loss; D - Excavated diameter of TBM Tunnel; i - Inflection point (m). For mostly cohesive soil the inflection point (i) is calculated by following;

$$i = KxZ_0 \tag{3}$$

Z_0 - Depth of tunnel (m); K - Coefficient, for soft clay it varies between 0.6 to 0.7

Using the O'Reilly and New [33] equation, the surface settlement is calculated for various lateral distances, and the transverse surface settlement trough for the 1st and 2nd tunnels is presented in Fig.10. The parameters (soil properties, tunnel geometry) that have been used during numerical modelling are used as the input data for the calculation of surface settlement.

The addition of two overlapping curves, as presented in Fig.10, defines the total/combined settlement for twin tunnels by superpositions. Fig.11 shows the variation of combined settlement with lateral distance. The maximum combined surface settlement is found to be 13.2 mm, and the observed settlement trough is almost similar to the normal distribution (Gaussian distribution curve) demonstrated by Peck [47].

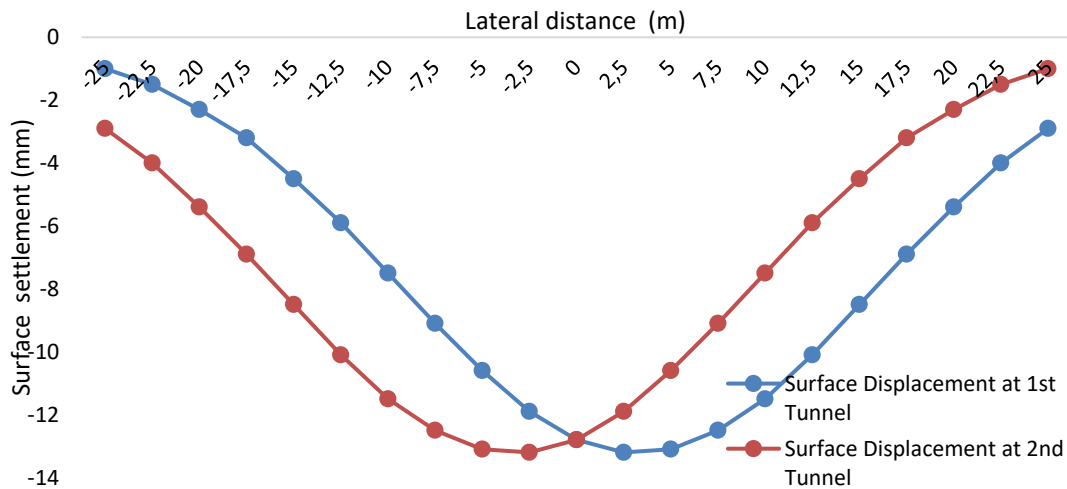


Fig. 10. Surface settlement trough for 1st and 2nd tunnel using O'Reilly and New method

Fig. 12 compares the combined surface settlement trough computed using numerical modelling (RS2) and the empirical equation proposed by O'Reilly and New [33]. The observed settlement trough of both techniques shows a similar pattern (Gaussian distribution curve) as observed in the analytical method proposed by Peck [47].

In the case of O'Reilly and New method, the maximum combined surface settlement is found to be 13.2 mm, whereas in the numerical method (RS2) it is to be 14.02 mm, which is closer to the empirical method and depicts a good agreement between the results. The O'Reilly and New method underestimate the surface settlement of error by 6%. This is because the empirical method ignores the effect of creep of ground and time-dependent consolidation [41]. But the small error of 6% is tolerable and can be minimized by considering the effect of ground creep and time dependent-consolidation, as well as by enhancing the modelling approach.

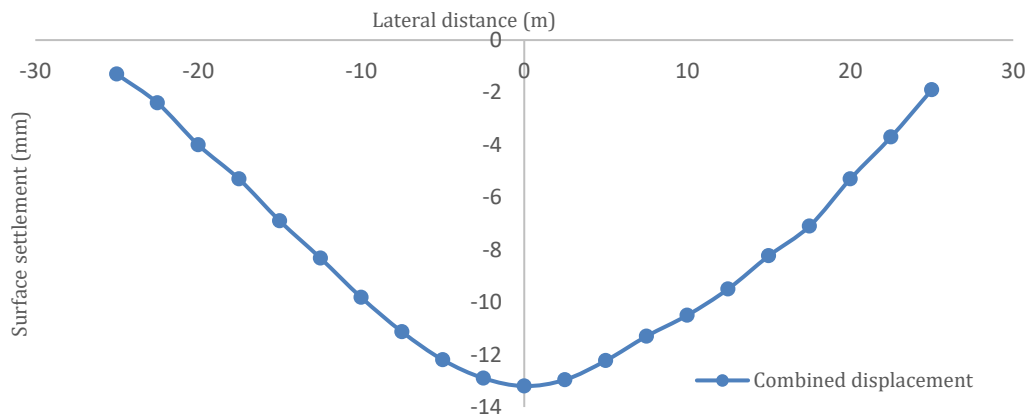


Fig. 11. Combined surface settlement trough for 1st and 2nd tunnel using O’Reilly and New method

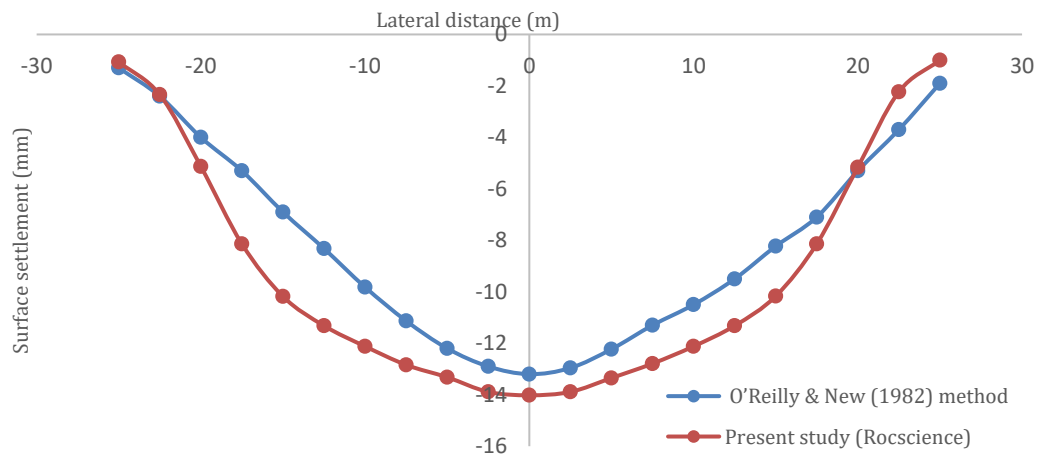


Fig. 12. Combined surface settlement trough for 1st and 2nd tunnel using numerical method (RS2) and O’Reilly and New approach

5.4 Surface Settlement Comparison with Analytical Studies

Several analytical methods have been used to predict tunnel induced surface settlement. Based on Peck’s [47] hypothesis that the settlement trough is a Gaussian distribution curve, the following three analytical methods are considered:

- Limanov’s method [50]
- Sagaseta’s method [51]
- Gonzales-Sagaseta method [52]

Table 5 shows the analytical equations and the calculated parameters required for each method, along with the results of the maximum surface settlement.

Table 5. Analytical equations and parameters required for each method with the results of the maximum surface settlement

Sr.No.	Method	Equation	Parameters					
1	Limanov's method	$S_{max} = (1 - \mu^2) \frac{P}{E} \left[\frac{4r_0 h}{(h^2 - r_0^2)} \right]$ $P = \sigma_z \times \frac{1 + k_s}{2}$	Tunnel depth (h) (m)	radius (r0) (m)	ks	P (kPa)	Smax (mm)	
			20	2.9	0.65	321	11.95	
2	Sagaseta's method	$S_{max} = \frac{VL \times D^2}{i}$	(h) (m)	VL (m3)	Smax (mm)			
			20	0.6	11.2			
3	Gonzales-Sagaseta method	$w(y) = 2 \epsilon r_0 \left(\frac{r_0}{h} \right) 2\alpha - 1x \frac{1}{1 + y^2} [1 + \rho \frac{1 + y^2}{1 - y^2}]$	ϵ	α	ρ	δ	u0 (mm) Smax (mm)	
			0.005	1.4	5.265	0.026	25 5.62	

Where; Ks- lateral earth pressure; P- radial load (kPa); E- radial shrinkage strain $\epsilon = \frac{u_0}{r_0}$; u0- uniform radial displacement; y-distance from the centerline; α -volume of compressibility ρ - relative ellipticity

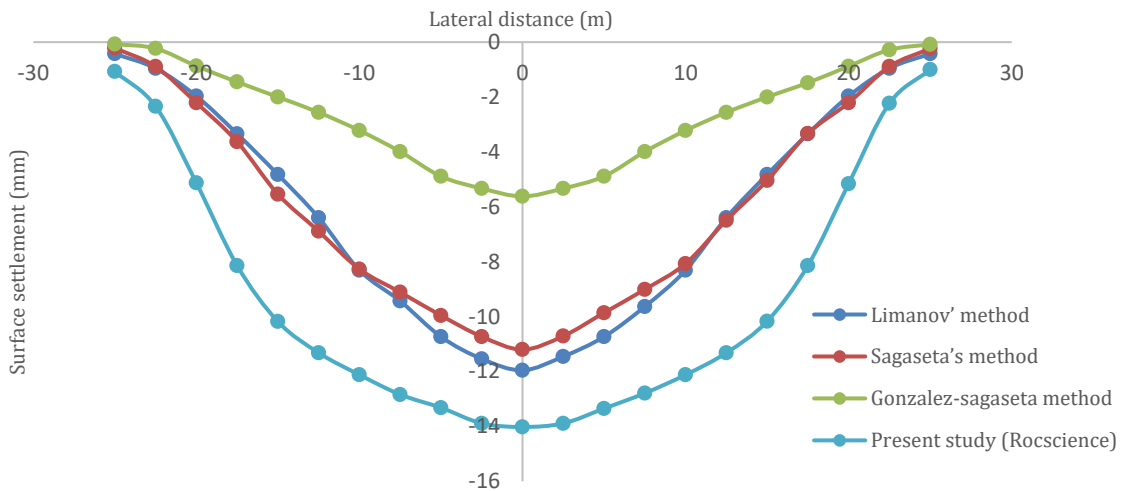


Fig. 13. Comparison of settlement trough obtained by various analytical methods with the present study (grouted water pocket)

The surface settlement trough observed using the numerical method (RS2) for the case of a grouted water pocket is compared with the abovementioned analytical methods. Fig.13 shows the comparison of the settlement trough obtained using various analytical methods and the profile obtained by the present study (RS2).

The settlement trough observed using various analytical methods and the numerical approach used in the present study exhibits a similar pattern with minor variation in the maximum surface settlement magnitude. This variation seen in the above analytical studies may be because of the assumptions and simplifications used when formulating the equations. The Gonzales-Sagaseta method underestimates the maximum surface settlement, which is almost 60% less than the present study result. While the surface settlements obtained using Limanov's and Sagasta's methods are 11.95mm and 11.2mm, respectively, which is close to the present study (14.2 mm).

Limanov’s and Sagasta’s methods show a small error of 15% and 21%, respectively, which is tolerable and can be minimized by enhancing the modelling approach.

5.5 Parametric Study

Tunnel surface settlement can be influenced by various parameters such as soil layer parameters (cohesion, frictional angle of resistance, unit weight, Young modulus, Poisson’s ratio), tunnel geometry (diameter and depth of tunnel), depth of water table, porewater pressure, support system, stress relaxation factor, etc. Chia Yu Huat et al. [53] concluded that the major parameters affecting the surface settlements are tunnel geometry, soil properties, tunnelling operation parameters, and tunnel center to center distance in the case of twin tunnels.

Many imperial and analytical methods focused on tunnel geometry and soil properties; very few methods considered the tunnelling operation parameters. In the present study, the effect of tunnel geometry (grouted tunnel), such as tunnel diameter and depth, on maximum surface settlement was evaluated and compared with the other methods while the other parameters were maintained constant.

5.5.1 Effect of Tunnel Diameter on Surface Settlement

To illustrate the effect of tunnel diameter on surface settlement, some calculations on different tunnel diameters, such as 5.0, 5.8, 7.0, 8.0, and 10.0m, are considered. The object of selecting the specific range of parameters was to compare how these parameters affected the maximum surface settlement. The RS2 analysis for maximum surface settlement was carried out for the above-specified range of tunnel diameters with a constant 20m overburden height, and the results were compared with the few analytical approaches tabulated in Table 6.

Table 6. Variation of tunnel diameter on maximum surface settlement

Sr. No.	Parameters			Maximum surface settlement (mm)			
	Diameter of tunnel D (m)	overburden height (h) (m)	h/D (m)	Present study (Rocscience)	Limanov’s method	Sagaseta’s method	Gonzales-Sagaseta method
1	5.0	20.0	4.0	13.43	10.64	10.07	5.33
2	5.8		3.45	14.02	11.95	11.2	5.62
3	7.0		2.85	17.01	16.7	14.1	8.46
4	8.0		2.5	19.7	21.2	17.4	10.7
5	10.0		2.0	24.4	26.33	22.9	17.2

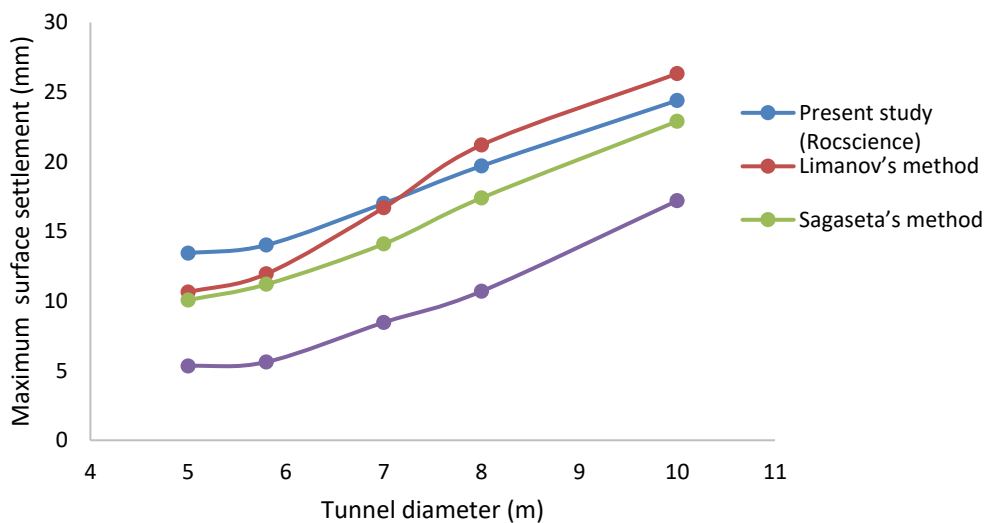


Fig. 14. Variation of tunnel diameter on maximum surface settlement and its comparison with analytical methods

From Fig 14, It is observed that the increase of tunnel diameter (D) significantly increases the maximum surface settlement; the same trend is also observed in analytical methods. These results are consistent with the findings [54,55,56]. This may be because a larger tunnel diameter displaces more volume of soil, consequently extending its influence zone. Within this area, soil undergoes stress redistribution, and this expanded region of stressed soil results in increased surface settlement [53].

In the present study, an increase of 81% in the maximum settlement has been found when the tunnel diameter increased from 5m to 10m. A similar effect was also observed in analytical methods, but the % of the increase in a settlement is more as compared to the present study (RS2). In Gonzales-Sagasetta method, the maximum settlement increased by 222% when the diameter of the tunnel increased from 5m to 10m. It indicates that decreasing the h/D ratio leads to an increase in the maximum surface settlement, but in Limanov’s method, as the h/D ratio reaches lower than 3.45, the difference in settlement increment becomes higher.

5.5.2 Effect of Tunnel Depth on Surface Settlement

Tunnel depth, also called overburden, is another one of the important parameters that influence surface settlement. Many researchers studied the overburden effect for a 5.0 m increment; hence in the present study, the surface settlement was calculated for a 5.0 m tunnel depth increment (5.0 m to 25 m) by maintaining the other parameters constant with the reference model. The present study results are also compared with the analytical methods, which are presented in Table 7 and Fig.15.

Table 7. Variation of tunnel depth (overburden) on maximum surface settlement

Sr. No.	Parameters			Maximum surface settlement (mm)			
	Overburden height (h) (m)	Diameter of tunnel D (m)	h/D (m)	Present study (Rocscience)	Limanov’s method	Sagasetta’s method	Gonzales-Sagasetta method
1	5.0		0.86	23.93	21.34	19.67	14.33
2	10		1.72	19.72	17.95	16.06	11.02
3	15	5.8	2.58	17.01	15.03	13.84	7.96
4	20		3.44	14.02	11.95	11.2	5.62
5	25		4.31	12.02	9.97	9.23	3.23

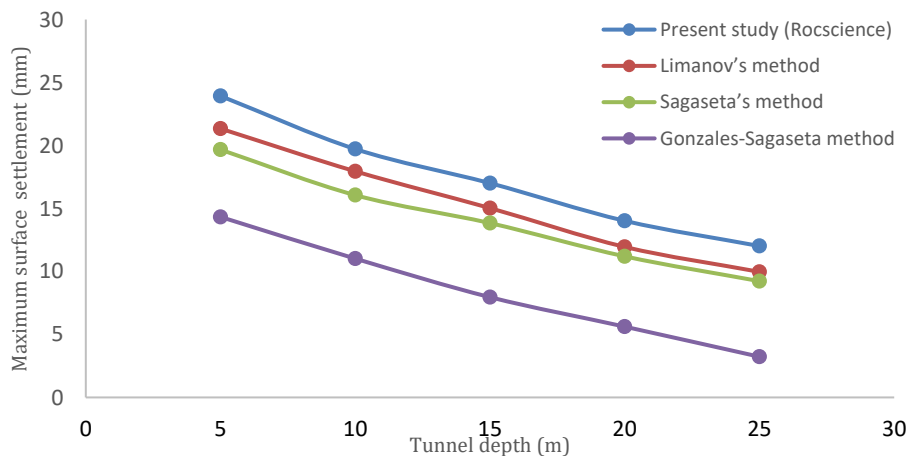


Fig. 15. Variation of tunnel depth on maximum surface settlement and its comparison with analytical methods

It is observed that an increase in tunnel depth (h) results in a significant decrease in maximum surface settlement. The observed findings are similar to the results obtained by previous studies [55,57,58,59]. Also, for an increase in the h/D ratio, the maximum surface settlement decreases. In

the present study, the maximum surface settlement was found to decrease by 99% when the depth of the tunnel increased from 5m to 25 m. The analytical methods also showed a similar pattern of results, but the % of reduction in surface settlement was higher as compared to the present study. Limanov's and Sagaseta methods show almost identical and close results to the present study, while Gonzales-Sagaseta method shows the maximum settlement decreased by more than 300% when the depth of the tunnel increased from 5m to 25.0m

6. Conclusion and Future Scope of Work

6.1 Conclusion

This paper estimates the twin- tunnel induced surface settlement trough using the numerical method (RS2) for the cases of TBM hits a water pocket (case A) and a grouted water pocket (case B) during the various tunnelling construction stages. The RS2 results were validated with the empirical method developed by O'Reilly and New method. Furthermore, the results were also compared with a few analytical approaches. To ascertain the applicability of RS2 method, a parametric study is also carried out for variation of tunnel geometry (depth and diameter). The following are the main conclusions of the present study:

- In the case of tunnel hits a water pocket, the maximum surface settlement was increased by 5% as compared to the 2nd tunnel excavation stage. This may be because entry of water in the excavation area increases the effective stress and consequently increases the surface settlement.
- In the case of grouted water pocket, the maximum surface settlement was found to be 16.4 mm, which is nearly 50% less than case A (the presence of water). This may be because of the pre-grouting effect of the water pocket, which controls the drawdown above the tunnel and reduces the effective stress, resulting in a decrease in the settlement.
- The support capacity curve shows that the liner factor of safety for case A is lower than the envelope value, indicating instability during the stage of the tunnel hitting the water pocket (saturated body), whereas, for case B, the liner's safety exceeds the design factor of safety. This demonstrates that once the water pocket is grouted, the tunnel segmental lining support will be safe.
- The surface settlement trough observed by RS2 shows a similar pattern (Gaussian distribution curve) to the O'Reilly and New method, also the maximum settlement values are found to be very close to the O'Reilly and New method with a deviation of 6% only.
- The RS2 results are compared with a few analytical approaches; the Gonzales- Sagaseta method underestimates the maximum surface settlement, while Limanov's and Sagasta's methods show close results with a deviation of 17% and 25%, respectively. This error may be tolerable and can be minimised by enhancing the modelling approach.
- A parametric study indicated that increasing the tunnel diameter from 5m to 10m resulted in an 81% increase in maximum surface settlement. A similar trend was observed in analytical methods, but the % increase in settlement was higher as compared to the present study (RS2).
- When the tunnel depth was increased from 5m to 25 m, a significant 99% decrease in the maximum surface settlement was observed. The analytical methods also showed a similar pattern of results. Limanov's and Sagaseta methods reveal 114% and 113% decrease in maximum surface settlement, respectively, which is almost close to the present study.

The proposed numerical method (RS2) has been validated with the empirical method and the results are also compared with analytical methods. Therefore, the RS2 can be used to calculate the surface settlement, particularly in the presence of a water/saturated body subject to the correct modelling approach. The use of predicted surface settlement guides the tunnel engineer about the future consequences of the destructive effects of adjacent structures and facilities.

6.2 Future Scope of Work

In the present study, the fictitious water pocket is positioned close to the 2nd tunnel crown. The position of water pocket/saturated bodies can be varied, and the influence on the surface

settlement can be studied. The present study results can be improved by using the more advanced models, such as Hardening Soil (HS) or Hardening Soil Small (HSs) models. The comparative study with the advanced model can be further studied. Also, the results can be verified using additional empirical, semi-empirical, or physical methods/ techniques.

Acknowledgements

The Management, Dr. Vishwanath Karad MIT World Peace University Pune is hereby acknowledged for providing the research facilities and permitting this research paper.

References

- [1] Klein S, O'Carroll J. Geotechnical risk assessments for tunnelling/underground projects. 2017: 350–359.
- [2] Nawani PC. Groundwater ingress in head race tunnel of Tapovan: Vishnugad Hydroelectric Project in Higher Himalaya, India. In Engineering Geology for Society and Territory 6. 2015: 941-945.
- [3] Anagnostou G. Tunnel stability and deformations in water-bearing ground. Eurock 06 ISRM Symposium on Multiphysics coupling and long-term behaviour in rock mechanics Liège (Belgium). 2012. May 9 – 12.
- [4] Liu Xialin. Predicting tunnel groundwater inflow by geological investigation using horizontal directional drilling technology. Advances in Civil Engineering. 2022:1-12. <https://doi.org/10.1155/2022/65783>.
- [5] Nikakhtar L, Zare S. Evaluation of underground water flow in to Tabriz metro tunnel first line by hydro-mechanical coupling analysis. World Academy of Science, Engineering and Technology International Journal of Geotechnical and Geological Engineering. 2020; (14) 01: 1-7. <https://doi.org/10.1155/2022/6578331>
- [6] Javadi M, Sharifzadeh M, Shahriar K. Uncertainty analysis of groundwater inflow into underground excavations by stochastic discontinuum method: Case study of Siah Bisheh pumped storage project, Iran. Tunneling and Underground Space Technology. 2016; 51:424-438. <https://doi.org/10.1016/j.tust.2015.09.003>
- [7] Wadslin Frenelus, Hui Peng, Jingyu Zhang. Evaluation methods for ground water inflows in to rock tunnels: a state of the art-review. International Journal of Hydrology. 2021; 5(4):152-168. <https://doi.org/10.15406/ijh.2021.05.00277>
- [8] Animateur EL. Settlement induced by tunnelling in soft ground. Tunneling and Underground Space Technology. 2007; 22: 119-149. doi:10.1016/j.tust.2006.11.001
- [9] Shin JH, Potts DM, Zdravkovic. Three-dimensional modelling of NATM tunnelling in decomposed granite soil. Geotechnique. 2002; 52 (3):187-200. <https://doi.org/10.1680/geot.2002.52.3.187>
- [10] Yoo Chungsik. Interaction between tunnelling and groundwater -numerical investigation using three-dimensional stress coupled analysis. Journal of Geotechnical and Geo environmental Engineering. 2005; 131(2):240-250. [https://doi.org/10.1061/\(ASCE\)1090-0241\(2005\)131:2\(240\)](https://doi.org/10.1061/(ASCE)1090-0241(2005)131:2(240))
- [11] Yoo C, Kim SB. Stability analysis of urban tunnelling in difficult ground condition. Tunneling and Underground Space Technology. 2006; 21(3-4):351-352. <https://doi.org/10.1016/j.tust.2005.12.170>
- [12] Jordi Font-Capo, Vazquez-Sune E, Carrera J, Herms I. Groundwater characterization of a heterogeneous granite rock massif for shallow tunnelling. Geologica Acta. 2012; 10 (4): 395 <http://dx.doi.org/10.1344/105.000001773>
- [13] Butscher C. Steady-state groundwater inflow into a circular tunnel. Tunneling and Underground Space Technology. 2012; 32:158-167. DOI: 10.1016/j.tust.2012.06.007
- [14] Yoo Chingsik, Lee Young Joo, Kim Sang-Hwan, Kim Hong-Taek. Tunnel induced ground settlements in a ground water drawdown environment-A case history. Tunneling and Underground Space Technology. 2012; 29: 69-77. <https://doi.org/10.1016/j.tust.2012.01.002>
- [15] Kong WK. Water ingress assessment for rock tunnels: A tool for risk planning. Rock Mechanics and Rock Engineering. 2011; 44:755-765. <https://link.springer.com/article/10.1007/s00603-011-0163-4>
- [16] Attewell PB, Yeates J, Selby AR. Ground deformation and strain equations. Soil Movements Induced by Tunneling and Their Effects on Pipeline and Structures. Glasgow: Blackie.1986: 53–66.
- [17] O'Reilly MP, Mair RJ, Alderman GH. Long-term settlements over Tunnels: An eleven-year study at Grimsby. In Tunnelling'91 London: Inst. of Mining and Metallurgy. 1991:55–64. <https://doi.org/10.1016/0148-9062%2892%2992317-6>
- [18] Bowers KH, Hiller DM, New BM. Ground movement over three years at the Heathrow Express Trial Tunnel. In Mair & Taylor (Eds.). Geotechnical aspects of underground construction in soft ground. 1996: 647–652.
- [19] Anagnostou G. Urban tunnelling in water bearing ground – Common problems and soil mechanical analysis methods. 2nd Int. conf. on Soil Structure Interaction in Urban Civil Engineering. Zurich. 2002: 233– 240

- [20] Shen SL, Wu HN, Cui YJ, Yin ZY. Long-term settlement behavior of the metro tunnel in Shanghai. *Tunneling and Underground Space Technology*. 2014; 40(1): 309–323. <https://doi.org/10.1016/j.tust.2013.10.013>
- [21] Shen SL, Tang CP, Bai Y, Xu YS. Analysis of settlement due to withdrawal of groundwater around an unexcavated foundation pit. *Underground Construction and Ground Movement*. 2006: 377–384. [https://doi.org/10.1061/40867\(199\)47](https://doi.org/10.1061/40867(199)47)
- [22] Xu YS, Shen SL, Bai Y (2006) State-of-art of land subsidence prediction due to groundwater withdrawal in China. *Underground Construction and Ground Movement*. 2006: 58–65. [https://doi.org/10.1061/40867\(199\)5](https://doi.org/10.1061/40867(199)5)
- [23] Shen SL, Xu YS. Numerical evaluation of land subsidence induced by groundwater pumping in Shanghai. *Canadian Geotechnical Journal*. 2011; 48(9):1378–1392. <https://doi.org/10.1139/t11-049>
- [24] Shen SL, Ma L, Xu YS, Yin ZY. Interpretation of increased deformation rate in aquifer IV due to groundwater pumping in Shanghai. *Canadian Geotechnical Journal*. 2013; 50(11): 1129–1142. <https://doi.org/10.1139/cgj-2013-0042>
- [25] Singh K, Mittal S, Kumar K. Reduction in lateral displacement of cohesionless soil box tunnel face using nails in overburden. *International Journal of Geosynthetics and Ground Engineering*. 2018; 4(21):1-21. <https://doi.org/10.1007/s40891-018-0138-6>
- [26] Ghorbani A, Hasanzadehshoili H, Eslami A, Shen W. Parametric evaluation of simultaneous effects of damaged zone parameters and rock strength properties on GRC. *Advances in Civil Engineering*. 2021 :1-13. <https://doi.org/10.1155/2021/2237918>
- [27] Likitlersuang S, Surarak C, Suwansawat S, Wanatowski D, Oh E, Balasubramaniam A. Simplified finite-element modelling for tunnelling-induced settlements. *Geotechnical Research*. 2014;1(4): 133-152. <http://dx.doi.org/10.1680/gr.14.00016>.
- [28] Bear J. *Dynamics of fluids in porous media*, Dover Publications, 1972: 1-757, ISBN 0-486-65675-6.
- [29] Akram MS, Noor A, Ullah MF, Ahmed L, Rehman F. Squeezing assessment along 2.84 km long headrace tunnel of a small hydropower project in KPK, Pakistan: Comparison of different methods: *International Journal of Geosynthetics and Ground Engineering*. 2019; 5(19):1-17. <https://doi.org/10.1007/s40891-019-0167-9>
- [30] Panji M, Ansari B. Transient S-H wave scattering by the lined tunnels embedded in an elastic half plane. *Engineering Analysis with Boundary Elements*. 2017; 84:220-230. <https://doi.org/10.1016/j.enganabound.2017.09.002>
- [31] Panji M, Ansari B. Anti plane seismic ground motion above twin horse shoe-shaped lined tunnels. *Innovative Infrastructure Solutions*. 2020; 5(7). <https://doi.org/10.1007/s41062-019-0257-5>
- [32] Ingle GS, Niphade S. Numerical and artificial neural network analysis of tunnel liner design parameters – a comparative study. *Geomechanics and Geoengineering*. 2024: 1–20. <https://doi.org/10.1080/17486025.2024.2354289>
- [33] O'Reilly MP, New BM. Settlement above tunnels in the United Kingdom- their magnitude and prediction. *Proceedings of the 3rd International Symposium Brighton*. 1983: 173-181. <https://doi.org/10.1016/0148-9062%2883%2991768-0>
- [34] Alsirawan R, Sheble A, Alnmr A. Two-dimensional numerical analysis for TBM Tunneling-induced structure settlement: A proposed modeling method and parametric study. *Infrastructures*. 2023; 8(5): 88. <https://doi.org/10.3390/infrastructures8050088>
- [35] Çelik S. Comparison of Mohr-Coulomb and hardening soil models numerical estimation of ground surface settlement caused by tunneling. *Iğdır Üni. Fen Bilimleri Enst. Der. / Iğdır Univ. Journal of the Institute of Science & Technology*. 2017; 7(4): 95-102. <http://dx.doi.org/10.21597/jist.2017.202>
- [36] Melis M, Medina L, Rodríguez, JM. Prediction and analysis of subsidence induced by shield tunnelling in the Madrid Metro extension. *Canadian Geotechnical Journal*. 2002; 39:1273–1287.
- [37] Möller SC. *Tunnel Induced Settlements and Structural Forces in Linings*. Doctoral Dissertation, Institute for Geotechnics, University of Stuttgart, Stuttgart, Germany, 2006.
- [38] Mroueh H, Shahrour I. A simplified 3D model for tunnel construction using tunnel boring machines. *Tunnelling and Underground Space Technology*. 2008; 23(1): 38-45. <https://doi.org/10.1016/j.tust.2006.11.008>
- [39] Migliazza M, Chiorboli M, Giani GP. Comparison of analytical method, 3D finite element model with experimental subsidence measurements resulting from the extension of the Milan underground. *Computers and Geotechnics*. 2009; 36 (1-2):113–124. <https://doi.org/10.1016/j.compgeo.2008.03.005>
- [40] Ocak I, Seker SE. Calculation of surface settlements caused by EPBM tunneling using artificial neural network, SVM, and Gaussian processes *Environmental Earth Sciences*. 2013; 70 (3): 1263-1276, [10.1007/s12665-012-2214-x](https://doi.org/10.1007/s12665-012-2214-x)
- [41] Gang N, Xuzhen He, Haoding Xu, Shaoheng Dai. Tunnelling-induced ground surface settlement: A comprehensive review with particular attention to artificial intelligence technologies. *Natural Hazards Research*. 2024; 4(1):148-168. <https://doi.org/10.1016/j.nhres.2023.11.002>

- [42] Mousivand M, Maleki M, Mansoori MR. Application of Convergence–Confinement Method in Analysis of Shallow Non-circular Tunnels. *Geotechnical and Geological Engineering*. 2017; 35:1185–1198. <https://doi.org/10.1007/s10706-017-0173-4>
- [43] Snežana Maraš-Dragojević. Analysis of ground settlement caused by tunnel construction. *GRAĐEVINAR*.2012;64(7):573-581. UDK: 624.193:624.131.54
- [44] De-Yang Wang, Hong-Hu Zhu, Xue-Hui Zhang, Jing-Wu Huang, Zhen-Rui Yan, Dao-Yuan Tan, Shao-Qun Lin. Structural behavior of triple-layer composite lining of a water conveyance tunnel: Insight from full-scale loading tests. *Journal of Rock Mechanics and Geotechnical Engineering*. 2024. In press. <https://doi.org/10.1016/j.jrmge.2024.11.025>
- [45] Nong Xingzhong, Liang Yuehua, Ruan Yanmei. A case study of deep shaft and open face tunnelling induced excessive ground settlement in water rich strata in Guangzhou China. *Frontiers in Earth Science* 10.2022. <https://doi.org/10.3389/feart.2022.825186>
- [46] Rankin WJ. Ground movements resulting from urban tunnelling: predictions and effects. Geological Society London, Engineering Geology Special Publications. 1988; 5(1): 79-92.<https://doi.org/10.1144/GSL.ENG.1988.005.01.06>
- [47] Peck RB. Deep excavations and tunnelling in soft ground. Proceedings 7th international Conference Soil Mechanics and Foundation Engineering Mexico State-of-the-Art Volume.1969: 225-290
- [48] Hansmire W, Cording E. Performance of a soft ground tunnel on the Washington Metro. In Proceedings of rapid excavation tunneling conference, Chicago.1972: 371–389.
- [49] Wang F, Miao L, Yang X M, Du Y J.The volume of settlement trough change with depth caused by tunneling in sands. *KSCE Journal of Civil Engineering*. 2016; 20(7): 2719–2724. <https://doi.org/10.1007/s12205-016-0250-x>.
- [50] Limaniv JA. Infolge Tunnelbau in kambrischen Tonen Leningrad Inst-Inzh. Zhelezu, Transport.1957.
- [51] Sagasetta C. Analysis of underground soil deformation due to the ground loss. *Geotechnique*.1987; 37(3):301-330
- [52] Gonzalez C, Sagasetta C.Patterns of soil deformations around tunnels application to the extension of Madrid Metro. *Computers and Geotechnics*. 2001; 28(6-7): 445-468. [https://doi.org/10.1016/S0266-352X\(01\)00007-6](https://doi.org/10.1016/S0266-352X(01)00007-6)
- [53] Chia Yu Huat, Danial Jahed Armaghani, Sai Hin Lai, Hossein Motaghedi, Panagiotis G Asteris, Pouyan Fakharian. Analyzing surface settlement factors in single and twin tunnels: A review study. *Journal of Engineering Research*. 2024.In Press. <https://doi.org/10.1016/j.jer.2024.05.009>
- [54] Kanagaraju R, Krishnamurthy P. Influence of tunneling in cohesionless soil for different tunnel geometry and volume loss under greenfield condition. *Advances in Civil Engineering*. 2020: 1–11. <https://doi.org/10.1155/2020/1946761>
- [55] Aswathy MS, Vinoth M, Mittal A. Impact of governing factors on prediction of tunneling induced surface settlement in young alluvium deposit. *Indian Geotechnical Journal*. 2022; 52: 13–27. <https://doi.org/10.1007/s40098-021-00561-4>
- [56] Agarwal J, Sarakar R. Greenfield settlements due to tunnelling using tunnel boring machine (TBM) in layered soils: a parametric study. *Sadhana, Indian Academy of Sciences*.2024;49 (75):1-12. <https://doi.org/10.1007/s12046-023-02425-4>
- [57] Attewell P B and Farmer I W. Ground disturbance caused by shield tunnelling in a stiff, over consolidated clay. *Engineering Geology*.1974; 8(4):361-381. [https://doi.org/10.1016/0013-7952\(74\)90028-3](https://doi.org/10.1016/0013-7952(74)90028-3)
- [58] Golpasand MR, Nikudel M, Uromeihy Ali. Specifying the real value of volume loss (V L) and its effect on ground settlement due to excavation of Abuzar tunnel, Tehran. *Bulletin of Engineering Geology and the Environment*. 2016 ;75: 485-501. <http://dx.doi.org/10.1007/s10064-015-0788-8>
- [59] Rezaei AH, Ahmadi Adli, Mohammad. The Volume Loss: Real estimation and its effect on surface settlements due to excavation of Tabriz Metro Tunnel. *Geotechnical and Geological Engineering*. 2020; 38: 2663–2684. <https://link.springer.com/article/10.1007/s10706-019-01177-5>.